

Final Report

E-20-E63  
#3

# Improved Photolytic Rate Measurements at PAMS Sites

Submitted by:

Air Quality Laboratory  
School of Civil and Environmental Engineering  
Georgia Institute of Technology  
Atlanta, GA 30332-0355

February 2004

**U.S. Environmental Protection Agency  
NCER  
Science to Achieve Results Program**

**EPA Grant Number:** R826772

**Title:** Improved Photolytic Rate Measurements at PAMS Sites

**Investigators:** Rodgers, Michael O., Pearson, James R.

**Institution:** Georgia Institute of Technology

**EPA Project Officer:** Shapiro, Paul

**Project Period:** March 22, 1999 through June 30, 2002

**Project Amount:** \$168,930

**RFA:** Air Pollution Chemistry and Physics (1998)

**Research Category:** Air - Chemistry, Physics & Engineering

Executive Summary .....	3
Objective .....	3
Summary/Accomplishments .....	4
Identification of Operational Requirements.....	4
Development of Prototype Instrument.....	4
Development of Data Processing Procedures .....	4
Field Tests of Prototype Instrument.....	6
Comparison of Measurements .....	8
Evaluation of Instrument Development .....	9
Introduction.....	10
Instrument Development.....	12
Design Requirements .....	12
Spectrometer .....	13
Optical Collection System .....	14
Data Collection System.....	17
Development of Data Processing Procedures .....	18
Whole Sky Camera .....	19
Field Test Site .....	20
Results and Discussion .....	22
Synopsis of Field Test Results.....	22
Typical Results.....	22
Measurement and Analysis Issues .....	30
Conclusions and Recommendations .....	32
References.....	33
Appendix: Typical TUV Model Conditions .....	39

U.S. Environmental Protection Agency  
NCER  
Science to Achieve Results Program

**EPA Grant Number:** R826772

**Title:** Improved Photolytic Rate Measurements at PAMS Sites

**Investigators:** Rodgers, Michael O., Pearson, James R.

**Institution:** Georgia Institute of Technology

**EPA Project Officer:** Shapiro, Paul

**Project Period:** March 22, 1999 through June 30, 2002

**Project Amount:** \$168,930

**RFA:** Air Pollution Chemistry and Physics (1998)

**Research Category:** Air - Chemistry, Physics & Engineering

## Executive Summary

### *Objective*

Traditionally, ambient atmospheric monitoring networks for regulatory purposes have focused on observing compounds of direct interest to human health and/or welfare. While these monitoring networks provide important information for risk assessments they normally lack the range of measurements necessary to evaluate why these pollutants are present at the observed concentration levels.

By contrast, the PAMS (Photochemical Assessment Monitoring Site) network aims at providing detailed information on the chemical composition of the urban atmosphere for use in the evaluation of the accuracy of photochemical transport models and in interpretive analysis of the chemistry of the urban atmosphere as well as more conventional regulatory purposes. Historically, a major limitation in the analysis and interpretation of data from PAMS and other similar networks has been an absence of reliable ultraviolet (UV) photochemical rates measurements at these locations. These photochemical measurements have been limited at PAMS since the necessary instrumentation has had a high acquisition and/or operational cost or was not designed for protracted unattended operation typical of these sites.

The principal objective of this project was to build, calibrate, field test and evaluate a prototype low-cost spectro-radiometer suitable for accurately measuring the most important lower atmospheric UV photolytic rates at PAMS sites. Further, this system was designed to be sufficiently robust to operate unattended for extended periods under conditions of minimal environmental control.



## **Summary/Accomplishments**

The overall program was divided into six phases. These were: 1) identification of detailed operational requirements; 2) design, construction and bench testing of the prototype instrument; 3) development of supporting algorithms and data analysis routines; 4) laboratory and field testing of the prototype instrument at an active PAMS site; 5) comparison of PAMS photochemical rate measurements with those from other instruments and model calculations and 6) modification, testing and evaluation of revised instrument and/or data analysis procedures. Results from each of these phases are summarized below.

### **Identification of Operational Requirements**

The photochemical rates selected for measurement by the prototype system were those showing the greatest importance for evaluation of fast photochemistry in urban areas. These are for ozone  $j(\text{O}^1\text{D})$ , nitrogen dioxide  $j(\text{NO}_2)$ , hydrogen peroxide  $j(\text{H}_2\text{O}_2)$ , nitric acid  $j(\text{HNO}_3)$ , nitrous acid  $j(\text{HONO})$ , formaldehyde ( $\text{CH}_2\text{O}$ ), methyl hydro-peroxide  $j(\text{CH}_3\text{OOH})$ , methyl nitrate  $j(\text{CH}_3\text{ONO}_2)$  and peroxy-acetyl nitrate jPAN. Among these rates, the requirements for spectral resolution of instrument (0.3 nm) were defined by those needed to determine  $j(\text{O}^1\text{D})$  and the upper measurement wavelength limit (410 nm) was established by that necessary to determine  $j(\text{NO}_2)$ .

### **Development of Prototype Instrument**

The general requirement for long-term unattended operation strongly discouraged the use of a scanning type instrument and thus only fixed grating type systems were considered. Continued improvements in both holographic UV gratings and large Charge-Coupled Device (CCD) detector arrays meant that the basic bandwidth and spectral resolution requirements could be met with relatively inexpensive 2048 element arrays and high throughput single-stage spectrometers. A variety of commercial spectrometers were evaluated and a fiber-coupled 0.2m crossed- Czerny-Turner (UV Holographic grating) system from Ocean Optics, Inc. (model S2000) was selected as the basis for the system.

To bring the light into the system three inlet systems were constructed for evaluation during the field phase. These were two diffuser-type (cosine) inlets (sintered quartz and UV polymer) and a quartz ball lens. Laboratory tests confirmed that the polymer inlet gave the best overall performance as was used for most of the field trials.

### **Development of Data Processing Procedures**

Collection of large quantities of spectra inevitably results in the collection of large volumes of data and the development of rapid and reliable data reduction techniques were essential. Accurate determination of low-light levels at high solar zenith angles (a weakness of the traditional Eppley™ TUVB UV radiometers and a prime motivating

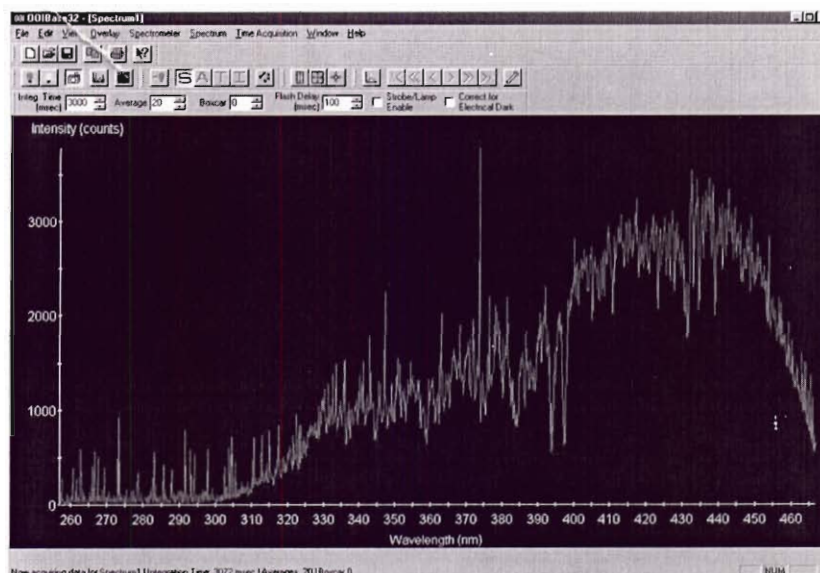
factor for the development of alternative UV measurement techniques) requires proper accounting for the impact of detector dark current on a pixel-by-pixel basis.

As detector dark current is principally a function of detector temperature, many systems provide for temperature control of the entire spectrometer system. This temperature control does, however, require additional power and provides another system failure point. Early in the development, it was decided to attempt to develop algorithms and techniques for correcting dark currents under conditions of widely varying temperatures. The rationale for this approach was that a correction algorithm effective over a wide range of temperatures could easily deal with constant temperature conditions but the converse would probably not be the case.

As part of this project an innovative internal referencing system was developed and tested. In this approach, under nocturnal conditions system dark currents are measured on a pixel-by-pixel basis throughout the night along with corresponding temperature data. During the day pixels below the tropospheric UV cutoff were monitored to record changes in dark current under generally higher temperature conditions typical of daytime. These data were combined to produce correction functions for individual pixels used for daytime measurements. Field test later verified that this approach could correct dark current to a relative error of less than 5% for temperature daily temperature fluctuations of up to 13 degrees Celsius. The success of this approach obviated the need for mechanical shutter systems for system blanking purposes in the prototype instrument.

Data reduction, including application of system calibration factors, was explored using several approaches. The first and most obvious approach was the use of commercial spectral analysis programs (e.g. Thermo Galactic's GRAMs™ software) or instrument control programs (e.g. Labtech Notebook™ or National Instruments Labview™ were both used during the project). While these systems worked well, their more general nature added significant cost to the overall system and less expensive solutions were evaluated. These included programming dedicated routines as well as the use spreadsheet macro programming (e.g. Microsoft Excel™). Ultimately, the final data analysis routines used for evaluation of the instrument were written as large macro programs in Microsoft Excel™ to minimize expense for potential end users. Data collection was made using the manufacturer's (Ocean Optics) data acquisition software. An example UV spectrum from the field testing program is given below:

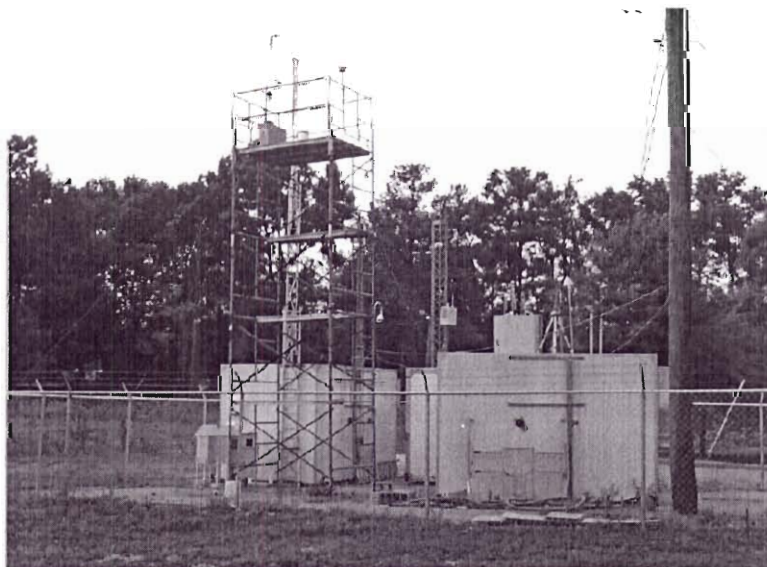




**Typical UV spectra collected as part of the field tests of prototype instrument**

### ***Field Tests of Prototype Instrument***

Initial field trials of the instrument were conducted during the summer of 1999. These were generally proof of concept tests and were not conducted with a complete system. During the second year (2000) the field tests of the prototype instrument were conducted at the Tucker, GA PAMS site. The instrument was operated for various periods from April through November at this site and collected more than 150,000 UV spectra during various testing programs. The figures below show the layout of the Tucker site. The spectroradiometer is located on the top of the immediately to the left of the meteorological system in the left center of the picture.



**Tucker, GA PAMS site used for field tests**

A more detailed view of the system is illustrated in the figure below. Two reference Eppley™ TUVB UV radiometer systems are visible to the left of the main spectrometer inlet on the top of the support column on the top right of the photograph. On the top of the main enclosure between the support columns is an inexpensive “whole sky” camera system also developed as a part of this effort. This system employs a low cost surveillance type digital camera and a hemispherical reflector. This system was used to estimate cloud coverage and type in support of modeling calculations. An illustration of a typical image from this system is also shown below. While this system proved useful for the semi-quantitative measurements for which it was intended, it was found to lack sufficient dynamic range to be generally useful unless equipped with an automatic iris.



**Figure: UV Radiometers and Spectrometer at Tucker, GA PAMS site**

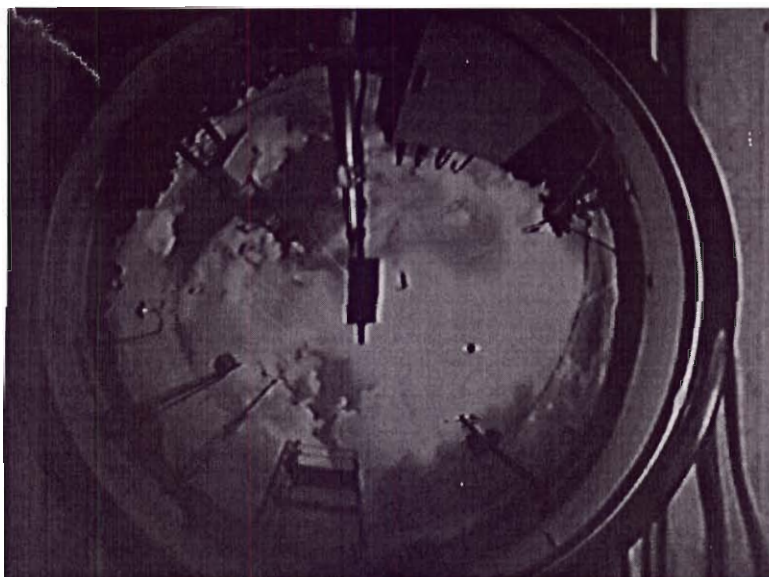


**Figure: Whole sky image from Tucker, GA PAMS site**

### ***Comparison of Measurements***

The final photochemical rates determined by the prototype system were in excellent agreement with a variety of multi-stream radiative transfer models from both the National Center for Atmospheric Research and Georgia Tech. However, achieving this good agreement required substantial post processing of the UV spectra. Automated processing of the data often resulted in sub-optimal baseline correction of the spectra leading to artifacts such as negative photolysis rates. An example of such an artifact is shown below for an exceptionally clear day in August 2000 at the Tucker PAMS site.

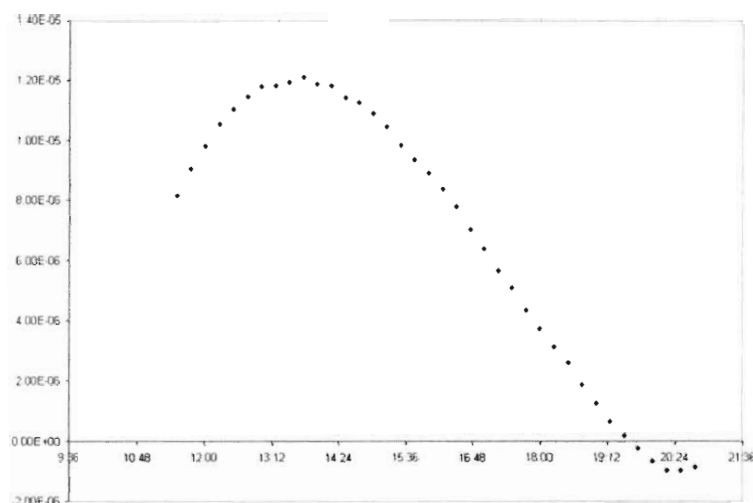


**Figure:  $J(O^1D)$  for Tucker, GA with Baseline Artifact**



The presence of such artifacts resulted in substantially more data analysis activity that would be desirable for system making routine measurements. At present, the analysis/time ratio (that is the ratio of time to analyze the data to running time) is about 0.05. That is, it takes approximately one hour of analyst time to process and quality-assure twenty hours of data. For full time deployment this corresponds to about 0.2 FTE (full time equivalents) of personnel per measurement site. At an annualized cost including overhead of \$100k/technician year this corresponds to an annual cost of \$20,000 per site.

## ***Evaluation of Instrument Development***

During 2001 and parts of 2002 additional tests were performed to optimize the instrumentation and procedures developed in the earlier test years. These modifications substantially improved the reliability of the hardware but resulted in less improvement in data analysis and reduction time. A summary of the principal finding and conclusions of the research program is given below:

- A reliable low cost and robust UV spectrophotometer based system for measurement of the most important photochemical rate coefficients has been built and tested.
- The measurements from this system are in good agreement with modeling calculations under clear sky conditions and with other measurement methods.
- Data handling and data processing time remain issues. The system generates more 50 Mb of data/day and data cannot be conveniently transmitted over conventional telephone lines. Even weekly data pickup requires high capacity (CD-R or greater) storage media.
- The system can be deployed and maintained at low annualized costs, however, at present the cost of data analyst time (\$20,000/site/year) will need to be reduced in order to make such photolytic measurements a routine part of the PAMS network.

## Introduction

Traditionally, ambient atmospheric monitoring networks for regulatory purposes have focused on observing compounds of direct interest to human health and/or welfare. While these monitoring networks provide important information for risk assessments they normally lack the range of measurements necessary to evaluate why these pollutants are present at the observed concentration levels.

By contrast, the PAMS (Photochemical Assessment Monitoring Site) network aims at providing detailed information on the chemical composition of the urban atmosphere for use in the evaluation of the accuracy of photochemical transport models and in interpretive analysis of the chemistry of the urban atmosphere as well as more conventional regulatory purposes. Historically, a major limitation in the analysis and interpretation of data from PAMS and other similar networks has been an absence of reliable ultraviolet (UV) photochemical rates measurements at these locations. These photochemical measurements have been limited at PAMS since the necessary instrumentation has had a high acquisition and/or operational cost or was not designed for protracted unattended operation typical of these sites.

Past research to determine the photolysis rates of atmospheric species can generally be divided into three main approaches, direct measurements of photolysis rates with chemical actinometers, derived photolysis rates from radiometric instruments and ultraviolet radiative transfer models (see for example: Dahlback and Stamnes, (1991), Ruggaber, et al. (1994), Madronich and Flocke (1998), Wild, et al. (2000)).

Only  $J(\text{NO}_2)$  and  $J(\text{O}^1\text{D})$  have been directly measured with chemical actinometers. The photolysis frequency of  $\text{NO}_2$  has been directly measured by Bahe, et al. (1980), Dickerson, et al. (1982), Harvey, et al. (1977), Huey (1993), Castro, et al. (1994), Parrish, et al. (1983), Zafonte, et al. (1977).

The photolysis rate of ozone has been measured directly by Bahe, et al. (1979), Dickerson, et al. (1979), Dickerson, et al. (1982), Hofzumahaus, et al. (1992), Bairai and Stedman (1992), Blackburn, et al. (1992).

Radiometric instruments have also been used to determine photolysis rates. Filter radiometers use different types of bandpass filters and a photocell to measure an actinic flux for a particular part of the UV spectrum. Photolysis rates are then calculated based on an empirical relationship. Spectroradiometers measure the actinic flux at each wavelength over the UV spectrum and integrate the flux, absorption cross section and quantum yield of each species to determine the photolysis rates. Radiometric measurements have been conducted by a variety of investigators (see for example Cotte, et al. (1997), Edwards and Monks (2003), Hofzumahaus, et al. (1999), Junkermann (1994), Kanaya, et al. (2003), Kazadzis, et al. (2000), Pfister, et al. (2000), Simpson, et al. (2002), Webb, et al. (2000), Webb, et al. (2003), Wiegand and Bofinger (2000), Wobrock, et al. (1988)).

Several studies have compared radiometric and chemical actinometers, Bais, et al. (2003), Cantrell, et al. (2003), Kraus and Hofzumahaus (2000), Kylling, et al. (2000), Madronich (1987), Muller, et al. (1995), Shetter, et al. (1992), Shetter, et al. (1996), Shetter, et al. (2003) and have generally concluded that the radiometric method has a broader range of applicability.

The principal objective of this project was to build, calibrate, field test and evaluate a prototype low-cost spectro-radiometer suitable for accurately measuring the most important lower atmospheric UV photolytic rates at PAMS sites. Further, this system was designed to be sufficiently robust to operate unattended for extended periods under conditions of minimal environmental control.

The overall program was divided into six phases. These were: 1) identification of detailed operational requirements; 2) design, construction and bench testing of the prototype instrument; 3) development of supporting algorithms and data analysis routines; 4) laboratory and field testing of the prototype instrument at an active PAMS site; 5) comparison of PAMS photochemical rate measurements with those from other instruments and model calculations and 6) modification, testing and evaluation of revised instrument and/or data analysis procedures. Results from each of these phases are summarized below.

# Instrument Development

## *Design Requirements*

As discussed earlier, there exists a need for improving photolytic rate measurements in support of atmospheric photochemical modeling and in interpretation of field measurement results. While chemical actinometers have been used for this purpose for many years, these systems typically measure only a few photochemical rates, have a high demand for consumables and require substantial operator intervention. On the other hand, modern spectroradiometers can measure a variety of photochemical rates with little consumption of consumables or operator intervention but require more elaborate calibration procedures. In addition, many of these “research grade” spectroradiometers are designed for “high performance” applications with high spectral resolution (normally  $<0.1$  nm in the UV) and often employ mechanical scanning systems that result in relatively high maintenance requirements.

The primary focus of this study was on the development and testing of a “de-contented” spectroradiometer that was designed to be very low in cost and highly reliable. Most of the cost saving were achieved by using substantially lower spectral resolution for the measurements that allowed for the use of single stage spectrometers using a fixed grating while still achieving sufficient bandwidth to measure most photochemical rates of significance in the troposphere. This trade-off was successfully achieved by careful evaluation of the actual resolution requirement for each of the measurements of interest. The photochemical rates selected for measurement by the prototype system were those showing the greatest importance for evaluation of fast photochemistry in urban areas. These are for ozone  $j(\text{O}^1\text{D})$ , nitrogen dioxide  $j(\text{NO}_2)$ , hydrogen peroxide  $j(\text{H}_2\text{O}_2)$ , nitric acid  $j(\text{HNO}_3)$ , nitrous acid  $j(\text{HONO})$ , formaldehyde ( $\text{CH}_2\text{O}$ ), methyl hydro-peroxide  $j(\text{CH}_3\text{OOH})$ , methyl nitrate  $j(\text{CH}_3\text{ONO}_2)$  and peroxy-acetyl nitrate  $j(\text{PAN})$ .

Initial analysis of the problem identified the measurement of rate of production of metastable atomic oxygen from ozone photolysis,  $j(\text{O}^1\text{D})$ , as the primary determinant of the minimum spectral resolution required for effective measurements. This is due to behavior of this system in the vicinity of 300 nm. Between 290 and 310 nm, the quantum yield for production of the metastable product drops rapidly with increasing wavelength while the absorption cross section for ozone is also declining significantly. On the other hand, the UV solar flux is increasing significantly with wavelength over this same region. Practically, this means that the overlap of solar flux, absorption cross-sections and quantum yields must be evaluated over relatively small wavelength intervals in order to achieve good results. Numerical simulations conducted early in project indicated that measurements made with a spectral resolution of 0.3 nm in this region would produce a  $<5\%$  error under near-worst case conditions compared to high-resolution measurements of the same quantities. This reduction in accuracy for this spectral resolution was deemed an acceptable design trade-off in terms of lowering system costs.



A similar analysis was conducted to establish the longest and shortest wavelengths required for the measurements (i.e. system bandwidth). The upper wavelength bound was found to be set by requirements for measurement of nitrogen dioxide photolysis ( $j(\text{NO}_2)$ ) at about 410 nm. The lower wavelength bound was established the minimum wavelength reaching the surface, about 280 nm.

## ***Spectrometer***

The heart of any system for spectroradiometric measurements is the spectrometer used for wavelength dispersion. Its selection is a critical element in design of the overall system and its performance will largely determine the ability of the system to operate successfully under field conditions. Field spectrometers need to be rugged and reliable and capable of operating unattended for periods of weeks to months. These requirements place severe limitations on the use of mechanically scanned devices and the selection process for the prototype system focused on fixed grating instruments that otherwise met the size, weight and cost criteria (target system cost of <\$20K). After evaluation of a number of competing instruments, the spectrometer chosen for use in the prototype instrument was a miniature fiber optic coupled spectrometer from Ocean Optics, Inc. (S2000).

The S2000 is a small and relatively inexpensive spectrometer that uses a crossed Czerny-Turner design in which light enters the spectrometer from a fiber optic cable through an entrance slit and is dispersed via a fixed grating across a detector array. The device finally chosen for incorporation into the prototype instrument employed 10  $\mu\text{m}$  wide slit as an entrance aperture and 1800 lines per mm, holographic UV-enhanced grating for wavelength dispersion. The typical spectral response of this grating is shown in Figure 1.

For measurement of the dispersed radiation, this prototype system was outfitted with a high sensitivity 2048-element linear silicon Charged-Coupled Device (CCD) array detector coated for use in the ultraviolet. This configuration yielded a system bandwidth of approximately 205 nm over the 260 – 465 nm wavelength interval. The dispersion is 0.10 nm/pixel and resolution is 3.2 pixels give the system an effective resolution of 0.32 nm. These criteria meet all of the primary design criteria established during the initial evaluations described above.

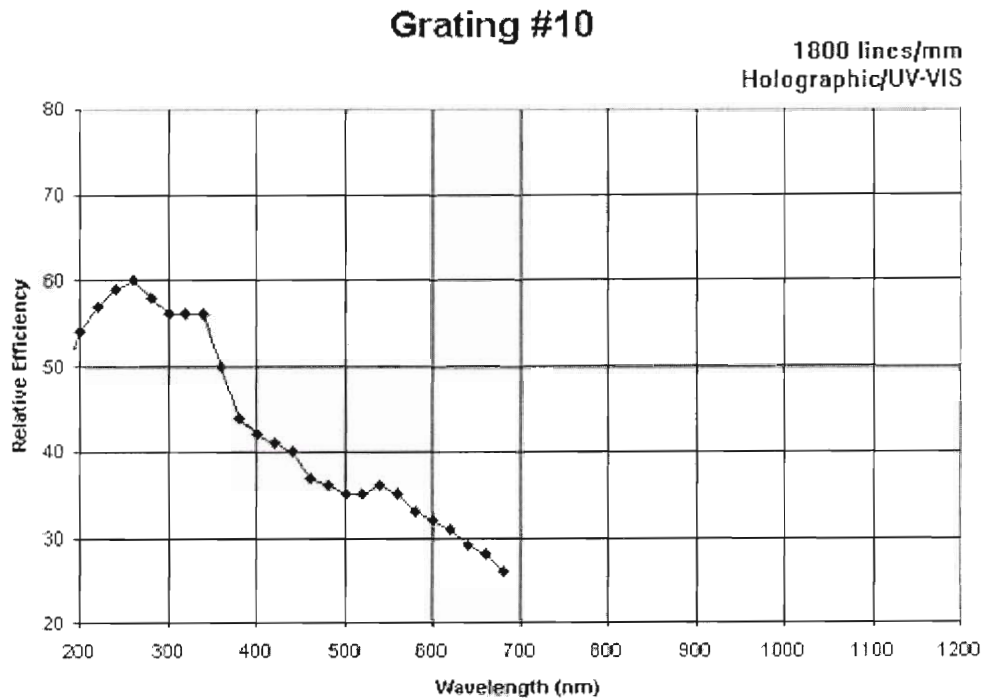


**Figure 1: Specified Grating Efficiency**

## ***Optical Collection System***

Of course, a spectrophotometer must also incorporate methods to quantitatively bring solar radiation into the system. The basic approach used in the prototype instrument is illustrated schematically in Figure 2. Light enters the system using a cosine-corrected light collection system located on a mast extending above a weather-protected housing that encases the spectrometer and electronics. This housing was thermostatically controlled using heaters and a cooling fan to improve measurement stability.

The cosine correction in the inlet system corrects for the natural variation of solar flux with zenith angle and significantly reduces corrections required in data post-processing. A UV fiber optic cable is used to bring the light from the collector to the entrance slit of the spectrometer. Use of fiber optic coupling reduces the angular dependence of the measurements and eases systems alignment. During development, three optical inlet systems were constructed for evaluation during the field phase. Two were diffuser type (cosine) inlets (sintered quartz and UV polymer) and other a quartz ball lens. Laboratory and early field tests confirmed that the polymer (Teflon®) inlet gave the best overall performance and was used for most of the field trials.

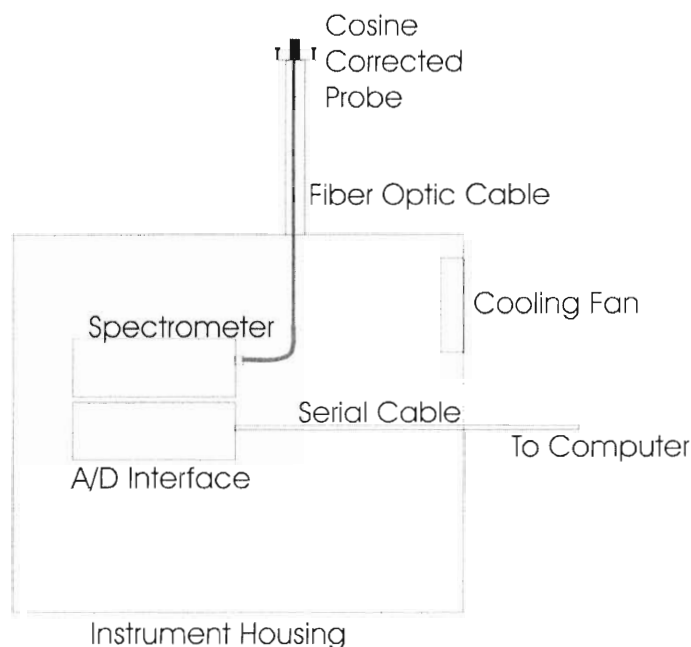


**Figure 2: Schematic Diagram of Instrument**

The primary field inlet system was based on a cosine-corrected fiber optic irradiance probe (CC-3-UV, Ocean Optics) with a 0.25" O.D. barrel and a black oxide finish modified to accept a thin Teflon® disk (7.5 mm thick) used as the diffusing material on one end of the probe. The other end of the probe used a Type 905 SMA connector for connection to a UV Fiber Optic Cable. This probe was mounted onto a 3" square flat mild steel plate with three adjustable screws for purposes of leveling. Since the inlet was coupled to the spectrometer through the fiber optic cable, this leveling could be conducted independently of the spectrometer. The inlet probe was mounted so as to protrude slightly (3 mm) from the plate to give the collector an  $\sim 180^\circ$  field of view. The angular response of the system is shown in Figure 3. Both the plate and the leveling screws were painted with a flat black paint to decrease the amount of stray light reflected into the probe.

The fiber optic cable used for all of the field data collection was a 2-meter long 100 $\mu\text{m}$  quartz fiber with a high OH fused silica core. This core was clad with a doped, lower refractive index fused silica layer that was itself surrounded with a polyimide coating. The fiber had an overall numerical aperture of 0.22 that gave an acceptance angle of  $24.8^\circ$ . The cable (Ocean Optics) was specifically designed for UV-VIS applications and was found to work well with no further modifications. A typical spectral attenuation is for the fiber is given as figure 4.

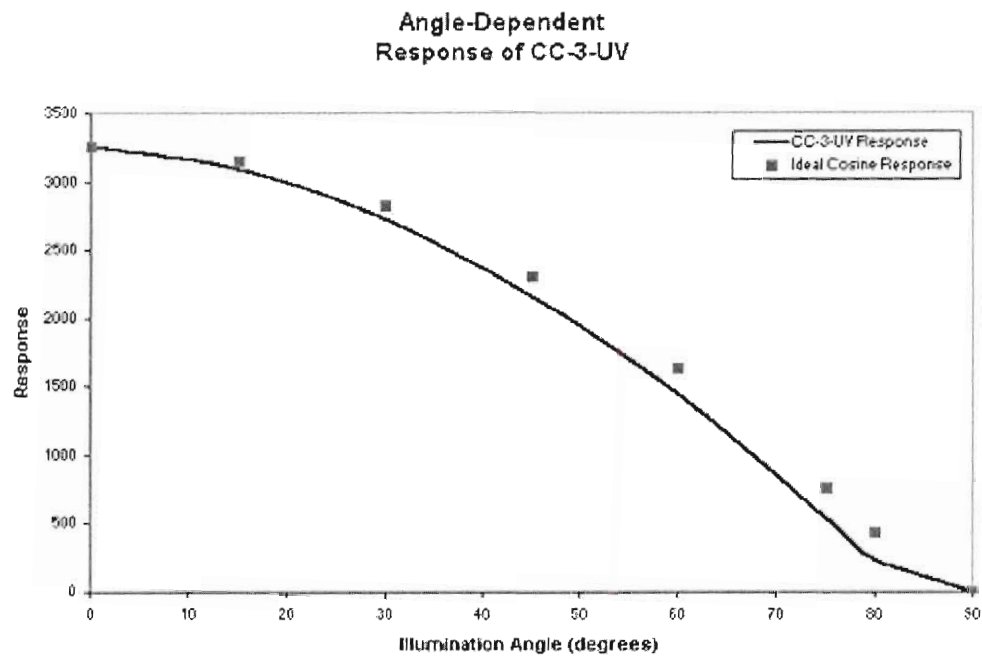


**Figure 3: Angular Response of Collection System**

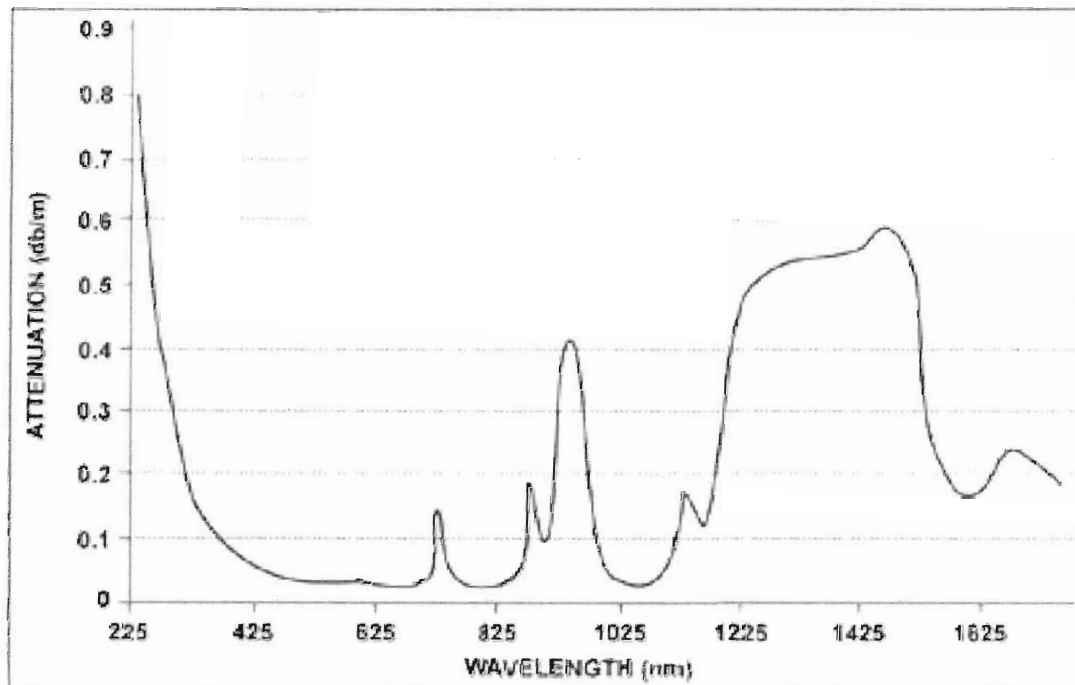


**Figure 4: Typical Attenuation of Fiber-Optic Coupling System (Ocean Optics)**



## Data Collection System

As illustrated in Figure 2, overall system control was maintained by external computer system. This system also controlled the whole sky camera as well as serving to collect ancillary data (e.g. TUV readings) used for data analysis or system comparisons. The spectrometer itself was controlled through a serial port interface (SAD500, Ocean Optics) in conjunction with this external computer. This interface incorporates a microprocessor-controlled A/D converter that communicated with the external computer system using the RS-232 protocol. System control and data collection from the spectrometer used the manufacturer's (Ocean Optics) supplied data acquisition software (OOIBase32). An example UV spectrum from the field-testing program is given in Figure 5:

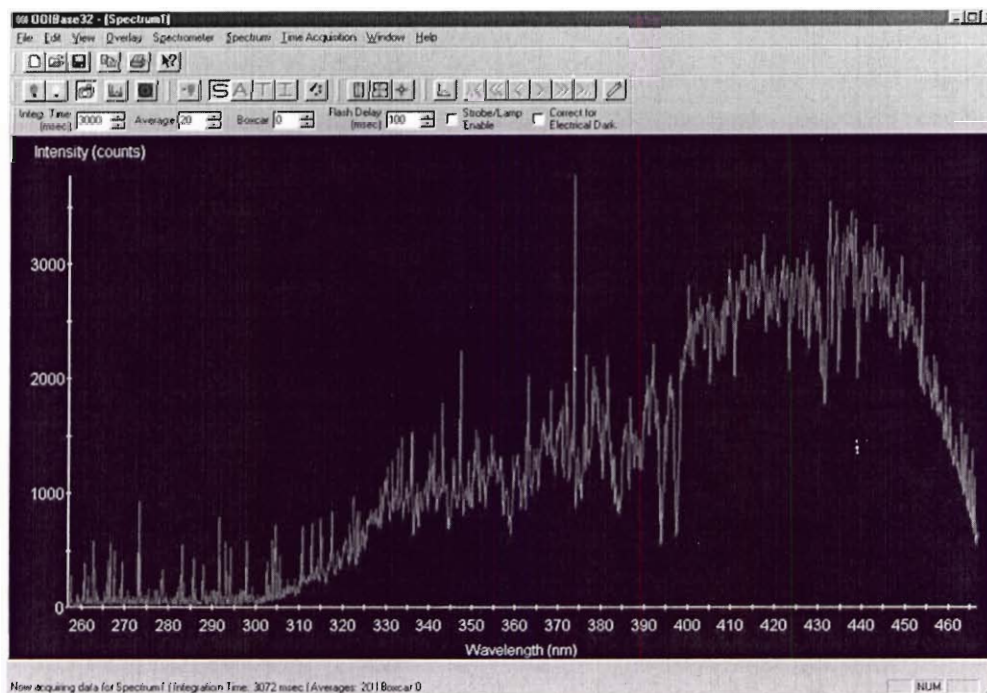


**Figure 5: Sample Solar Spectra from Tucker, GA Field Site**

The data shown in figure 5 is in the “scope” mode of the software in which the digitized voltages from each pixel from the A/D converter are given as a function of wavelength.. This spectral view allows adjustment of the signal processing functions before beginning a measurement cycle. In this mode, the effect of the intensity of the solar radiation, the reflectivity of the grating and mirrors in the spectrometer, the transmission efficiency of the fibers, the responses of the detectors are all shown before corrections are applied.

A typical application was the setting of the system integration time (dwell time per channel) that determines the number of milliseconds that receiving light before being read. The integration time varied by time of year and was set to give an optimum

response of 3500-4000 counts per channel at solar noon. Each individual spectrum within the data collection period was averaged to produce a composite spectrum was stored for later analysis. The number of spectra that were averaged to produce this composite spectrum varied with the system integration time and the data collection time period. For example, if the integration time was 2000 msec and the data collection period was 1 minute then 30 spectra are averaged to produce the composite stored spectra. Each of these composite spectra acquired by the system it is written to external computers hard disk using a sequential filename tied to the data collection period.

## ***Development of Data Processing Procedures***

Collection of large quantities of spectra inevitably results in the collection of large volumes of data and the development of rapid and reliable data reduction techniques were essential. Accurate determination of low-light levels at high solar zenith angles (a weakness of the traditional Eppley™ TUVB UV radiometers and a prime motivating factor for the development of alternative UV measurement techniques) requires proper accounting for the impact of detector dark current on a pixel-by-pixel basis.

As detector dark current is principally a function of detector temperature, many systems provide for temperature control of the entire spectrometer system. This temperature control does, however, require additional power and provides another system failure point. Early in the development, it was decided to attempt to develop algorithms and techniques for correcting dark currents under conditions of widely varying temperatures. The rationale for this approach was that a correction algorithm effective over a wide range of temperatures could easily deal with constant temperature conditions but the converse would probably not be the case.

As part of this project an innovative internal referencing system was developed and tested. In this approach, under nocturnal conditions system dark currents are measured on a pixel-by-pixel basis throughout the night along with corresponding temperature data. During the day pixels below the tropospheric UV cutoff were monitored to record changes in dark current under generally higher temperature conditions typical of daytime. These data were combined to produce correction functions for individual pixels used for daytime measurements. Field test later verified that this approach could correct dark current to a relative error of less than 5% for temperature daily temperature fluctuations of up to 13 degrees Celsius. The success of this approach obviated the need for mechanical shutter systems for system blanking purposes in the prototype instrument.

Data reduction, including application of system calibration factors, was explored using several approaches. The first and most obvious approach was the use of commercial spectral analysis programs (e.g. Thermo Galactic's GRAMS™ software) or instrument control programs (e.g. Labtech Notebook™ or National Instruments Labview™ were both used during the project). While these systems worked well, their more general nature added significant cost to the overall system and less expensive solutions were evaluated. These included programming dedicated routines as well as the use spreadsheet

macro programming (e.g. Microsoft Excel™). Ultimately, the final data analysis routines used for evaluation of the instrument were written as large macro programs in Microsoft Excel™ to minimize expense for potential end users. These macro programs are provided in the supplemental data DVD available with this report.

### ***Whole Sky Camera***

A major influence on actinic flux measurements is the amount and type of cloud cover present in the area. In order to evaluate the cloud conditions, a whole sky camera system was designed to compliment the spectroradiometer measurements. A miniature, low-resolution (320 x 240 pixels) surveillance-type video camera (Xcam from X10, Inc.) was used to record sky images. The camera was mounted above a full dome (hemispherical) mirror to provide a 360° view of the sky. The output of the video camera was sent to a USB video capture adapter and then to the external control computer. The image capture software (Xray Vision from X10) captured a single image every 2 minutes and stored the picture in a binary file. The files were later extracted and saved as individual jpeg images. An example of the sky cam view is shown in the figure 6. This system was used to estimate cloud coverage and type in support of modeling calculations as part of the field study program. While this system proved useful for the semi-quantitative measurements for which it was intended, it was found to lack sufficient dynamic range to be generally useful unless equipped with an automatic iris.

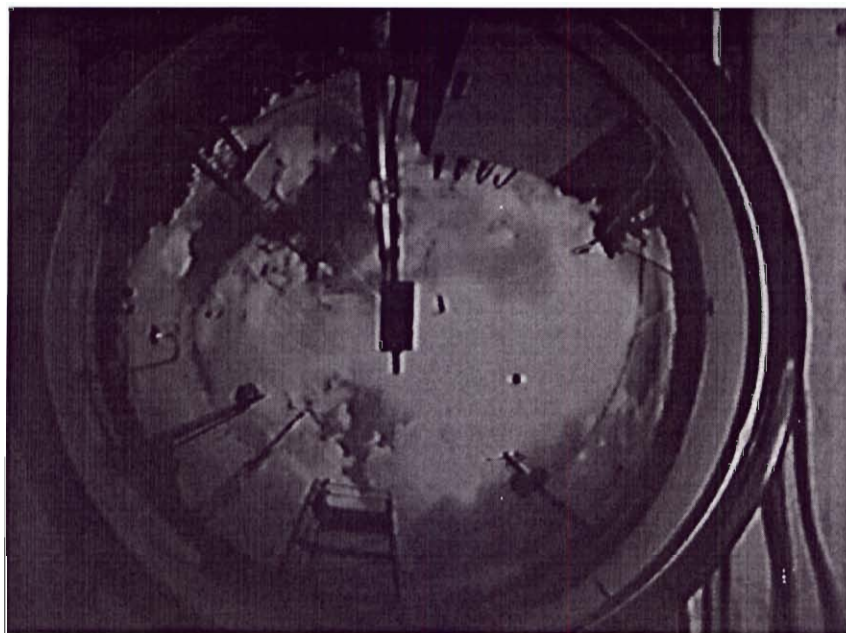


**Figure 6: Whole Sky Camera Image from Tucker, GA PAMS Site**



## Field Test Site

All initial laboratory and field evaluations of the instrument during the first year of the program (1999) were conducted on the campus of Georgia Institute of Technology located in mid-town Atlanta, GA. After development of the initial version of the prototype instrument a series of field trials were conducted during the second year (2000) of the program. These tests were aimed at establishing the performance and reliability of the system as well as its ability to operate unattended in typical field measurement setting. These trials were conducted at the Tucker, GA PAMS site. The Tucker PAMS site is located in a suburb about 25 km northeast of downtown Atlanta and was one of the first PAMS sites established. Figure 7 shows the location of the site.



**Figure 7: Location of the Tucker, GA PAMS Site. This site was the location of all of the field performance tests conducted during 2000.**

The prototype instrument was operated at this site for various periods from April through November and collected more than 150,000 UV spectra during various testing programs totaling approximately 110 days of data. Figure 8 gives a photograph of the Tucker site as configured for the testing program. In Figure 8, the prototype spectroradiometer is located on the top of the scaffolding immediately to the left of the meteorological system in the left center of the picture. Figure 9 shows a close up view of the system with the instrument enclosure opened. The Eppley TUVB® systems used for comparison with the spectroradiometer and the whole sky camera are also illustrated.



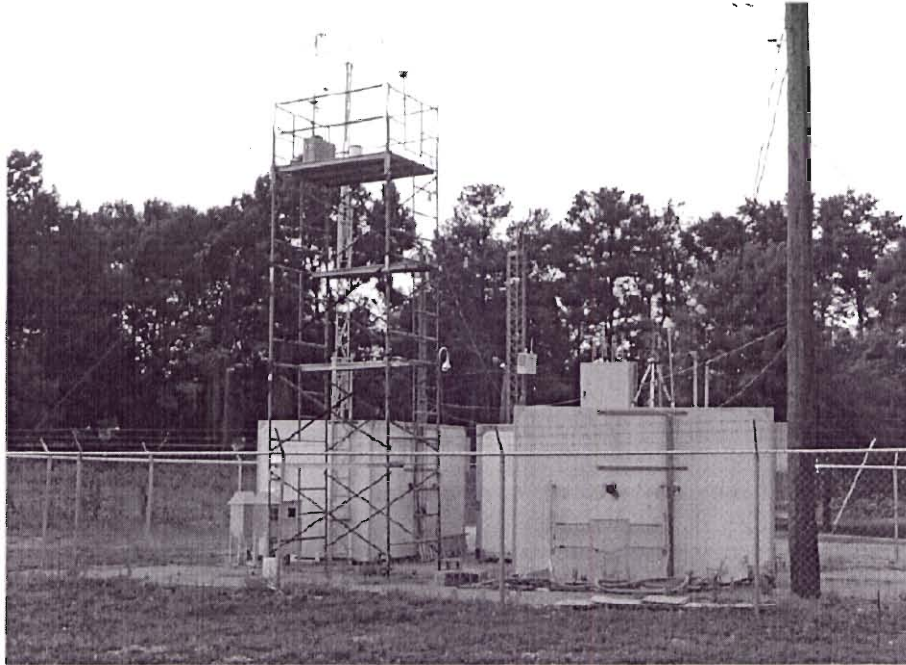


**Figure 8: Tucker, GA PAMS site used for field tests. The spectroradiometer is located on the scaffolding in the left center of the picture immediately adjacent to the meteorological system.**



**Figure 9: UV Radiometers and Spectrometer at Tucker, GA PAMS site.**

## **Results and Discussion**

### ***Synopsis of Field Test Results***

Data were collected on 110 days in the spring, summer and fall of 2000. This test program resulted in the collection of more than 150,000 spectra totaling more than 5 Gigabytes of stored data. These data are available in DVD form as a supplementary disk to this report. Since the purpose of the field tests was instrument development rather than consistent data collection, significant data gaps in this record are present when the system was down for repairs and/or system modification. During the field test period, by far the largest amount of unscheduled system downtime was as a result of problems with the external control computer system and/or its associated software. These problems collectively represented more than 90% of all unscheduled downtime. Most of these problems were associated with system “freeze-ups” associated with the multiple programs running on the main computer. These conflicts typically resulted in suspension of data collection and/or storage and generally required a system restart. Replacement of the computer system with a more capable machine in 2001 resulted in significantly improved performance in this area.

The spectroradiometer itself proved highly reliable and represented only an occasional problem in terms of data collection. The system did prove to have some significant operational difficulties associated with bird activity. Many local and migratory birds found the inlet probe to the spectroradiometer a convenient perch and depending, upon the inclinations of the bird, could inhibit measurements briefly or for extended periods.

### ***Typical Results***

In this section we will provide some typical results for the prototype instrument to illustrate some of its capabilities and limitations. Figure 10 contrasts photolysis rate measurements between a cloudy day (June 4<sup>th</sup>, top) and a mostly sunny day (July 17<sup>th</sup>, bottom). On July 17<sup>th</sup> the morning and early afternoon were sunny while the afternoon had scattered cloudiness. This figure illustrates the substantial deviation from theoretical photolysis rates in the presence of substantial cloud cover.

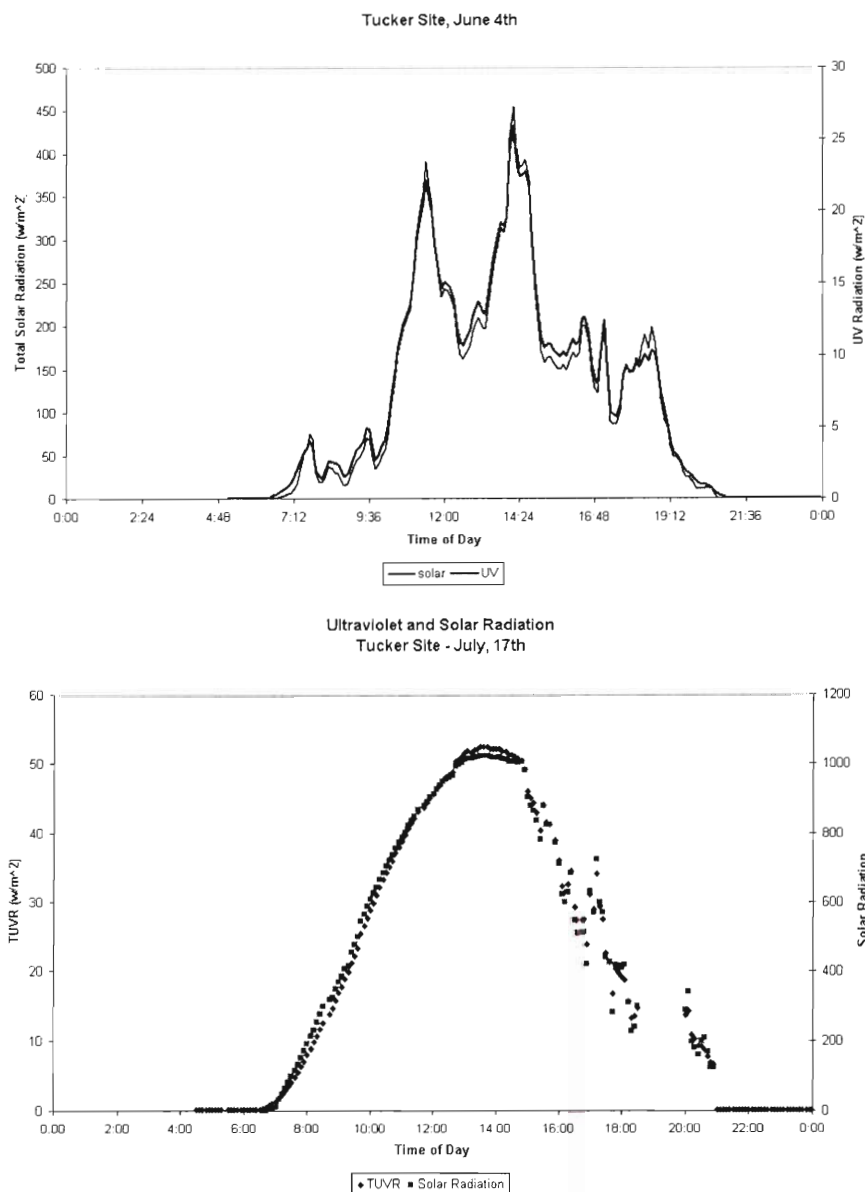
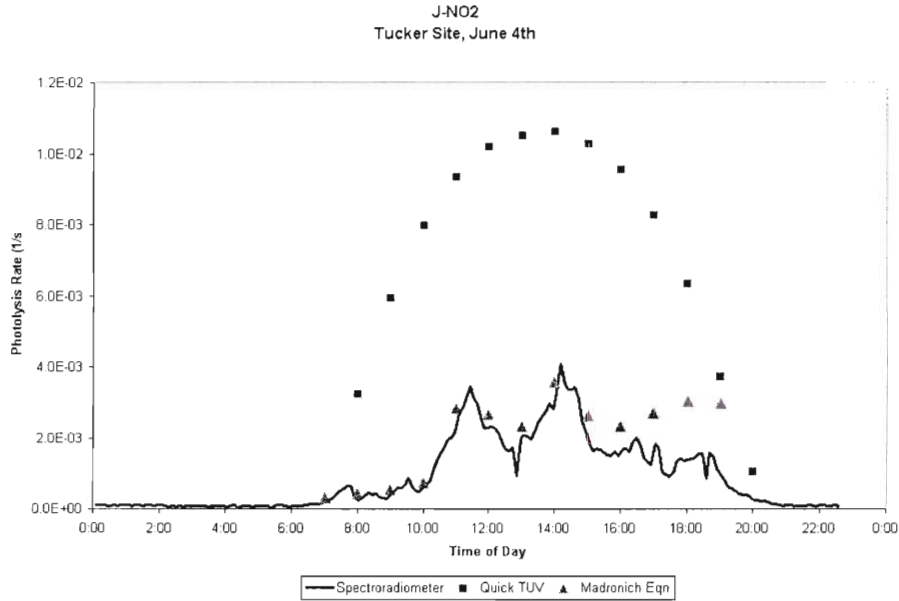


**Figure 10: Comparison of Photolytic Rates between a Cloudy Day (June 4, 2000, top graph) and a Mostly Clear Day (June 17, 2002, bottom graph) at Tucker, GA**

The photolysis rates calculated from the spectroradiometer measurements are compared to the rates that are calculated with the Tropospheric Ultraviolet and Visible Radiation Model (TUV) for the cloudy day (June 4) are given in Figure 11. The TUV model is a pseudo-spherical discrete ordinate four stream model that calculates 56 different photolysis rates based on the following inputs: date, time, latitude, longitude, overhead ozone column, surface albedo, ground elevation and measurement altitude. The photolysis rate for  $\text{J}(\text{NO}_2)$  can also be estimated from an empirical expression of Madronich (1987). A typical TUV model input file is given as an Appendix.

$$J(NO_2) \approx \frac{1.35 * E}{(0.56 + 0.03Z) \cos \chi_o + 0.21}$$

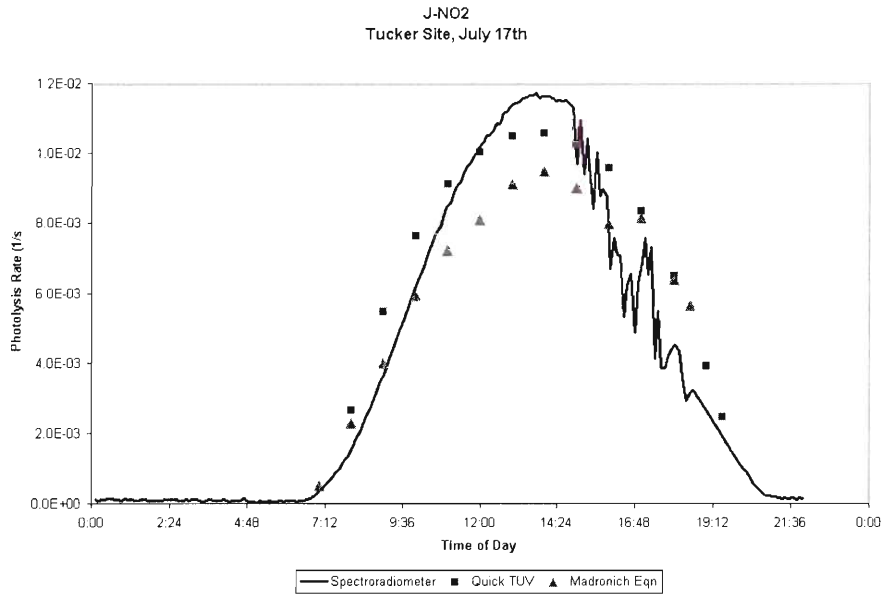
E is the ultraviolet radiation from an Eppley TUVB ® measured in W/m<sup>2</sup>, Z is the elevation above sea level in km, and  $\chi_o$  is the solar zenith angle.



**Figure 11: Comparison of Theoretical, Semi-empirical and Measured Nitrogen Dioxide Photolytic Rates for a Cloudy Day**

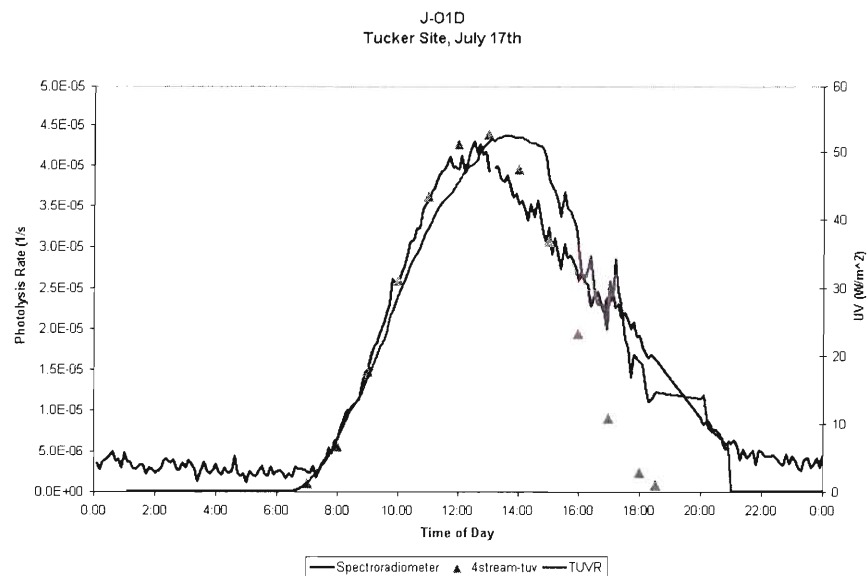
The figure above shows the calculated values for  $J(NO_2)$  on an overcast day, June 4, 2000. The TUV model results are much higher than the values from the spectroradiometer or the Madronich Equation since the model does not take cloud cover into account. Since the Madronich Equation is derived from the TUVB data it is in better agreement with the data from the spectroradiometer. The empirical relationship of the Madronich Equation tends to break down at high solar zenith angles and this can be seen in the early evening hours on June 4<sup>th</sup>. Figure 12 shows the calculated  $J(NO_2)$  values during the mostly sunny day on July 17<sup>th</sup>. In this case, there is generally good agreement between the model and the measurements.





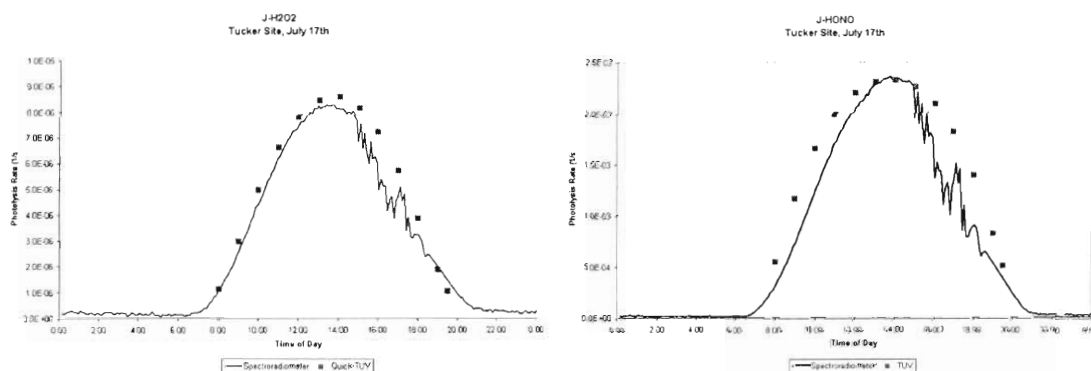
**Figure 12: Comparison of Theoretical, Semi-Empirical and Measured Nitrogen Dioxide Photolysis Rates for a Mostly Sunny Day**

Figure 13 below shows  $J(O^1D)$  values from the spectroradiometer and the TUV model output with the empirical measurements from the TUVR instrument. There is good agreement with the model in the morning and early afternoon but some disagreement in the late afternoon. This is likely caused from light scattering and light reflection under the developing clouds. This additional light is also seen by the TUVR instrument but not reflected in the model output. This leads to higher  $J(O^1D)$  values in the evening hours.



**Figure 13: Comparison of Ozone Photolysis Rates**

The measurements are also shown to be in good agreement with the model estimates under sunny conditions for both  $J(\text{H}_2\text{O}_2)$  and  $J(\text{HONO})$  shown in Figure 14 below.



**Figure 14: Comparison of Measured and Modeled Photolysis Rates for Hydrogen Peroxide and Nitrous Acid**

Figures 15, 16 and 17 show  $J(\text{PAN})$ ,  $J(\text{HNO}_3)$ , and  $J(\text{CH}_3\text{COOH})$  during a mostly sunny day in contrast to the results from Figure 14, the measured values are consistently lower than the model results except for the late afternoon.

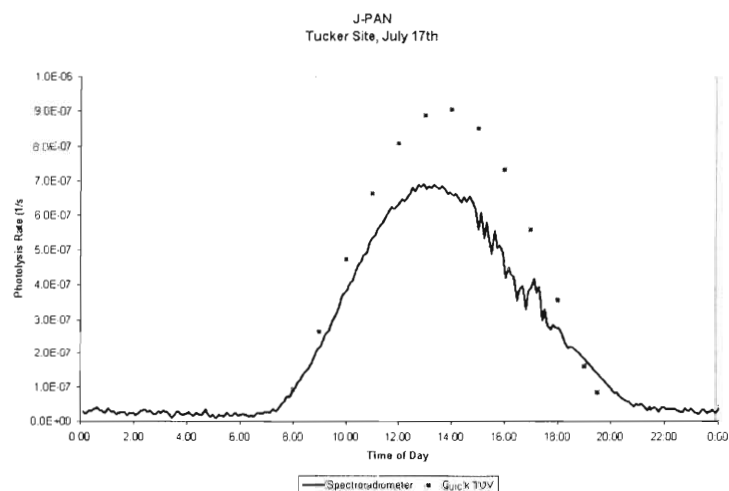


**Figure 15: Measurements and Modeled  $J(\text{PAN})$  for a Mostly Sunny Day**

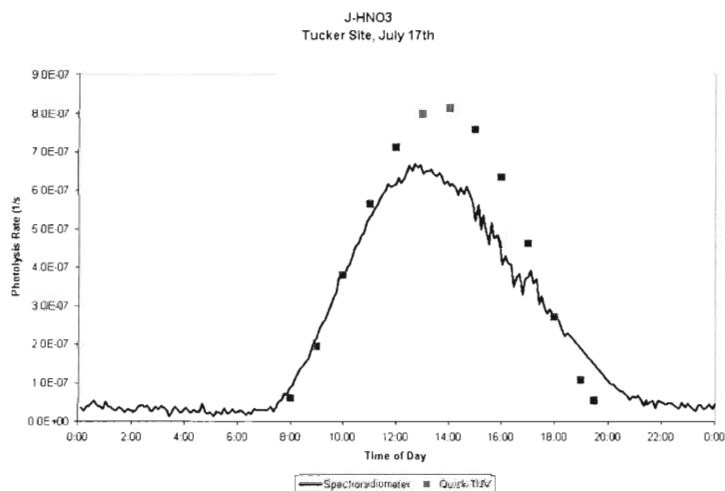


**Figure 16: Measured and Modeled Photolysis Rates for Nitric Acid for Mostly Sunny Conditions**

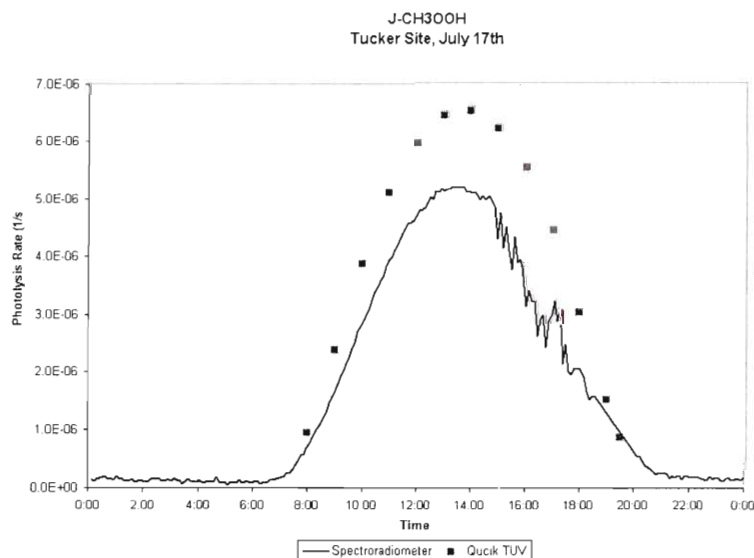
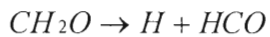


**Figure 17: Measured and Modeled Photolysis Rates for Methyl-Hydro Peroxide**

During photolysis, formaldehyde branches into two different channels. The first channel leads to radical formation,



while the second channel leads to more stable end products,

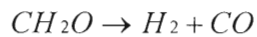
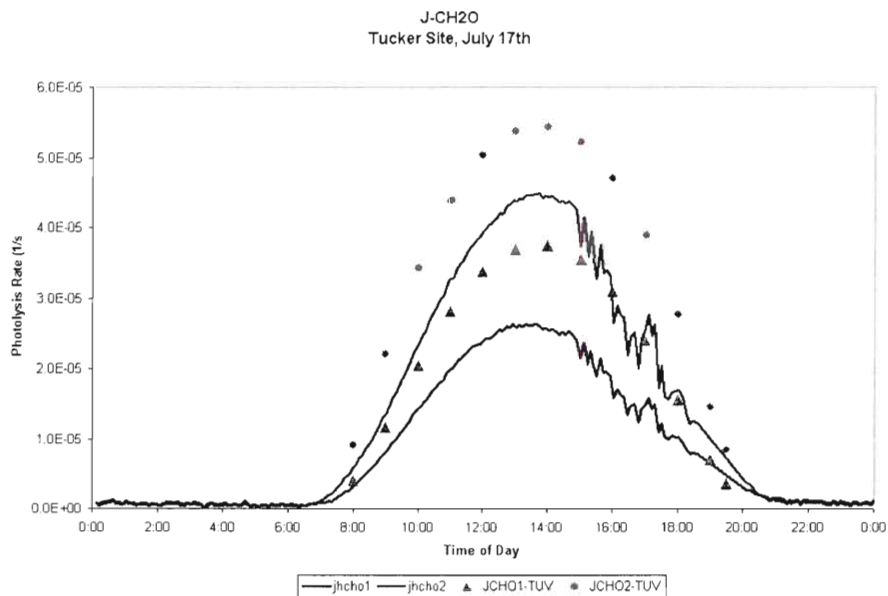
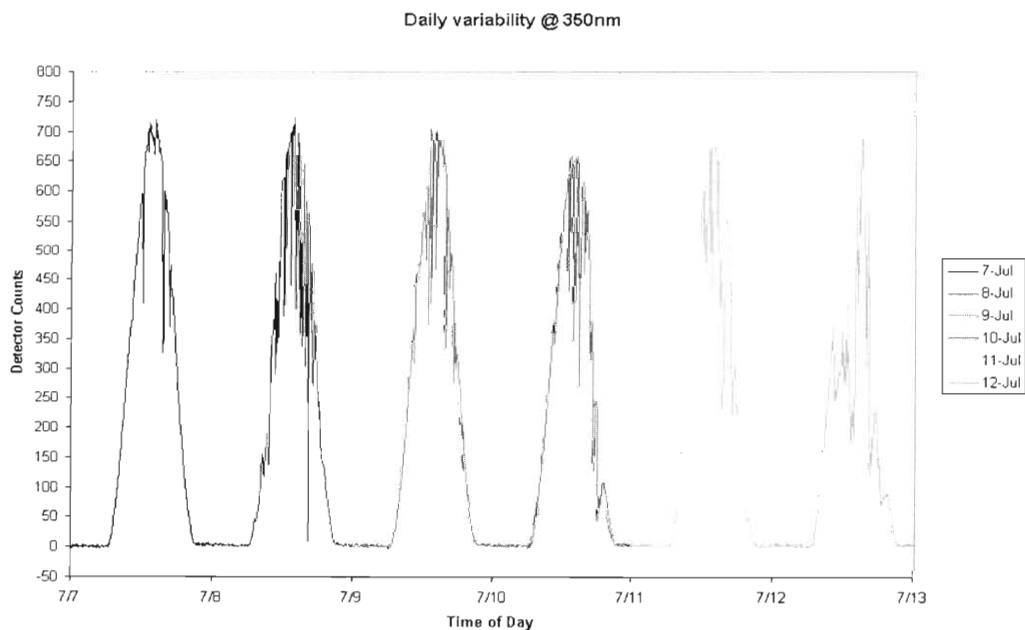


Figure 18 shows the photolysis rates for both channels compared to model results.



**Figure 18: Formaldehyde Photolysis Rates**

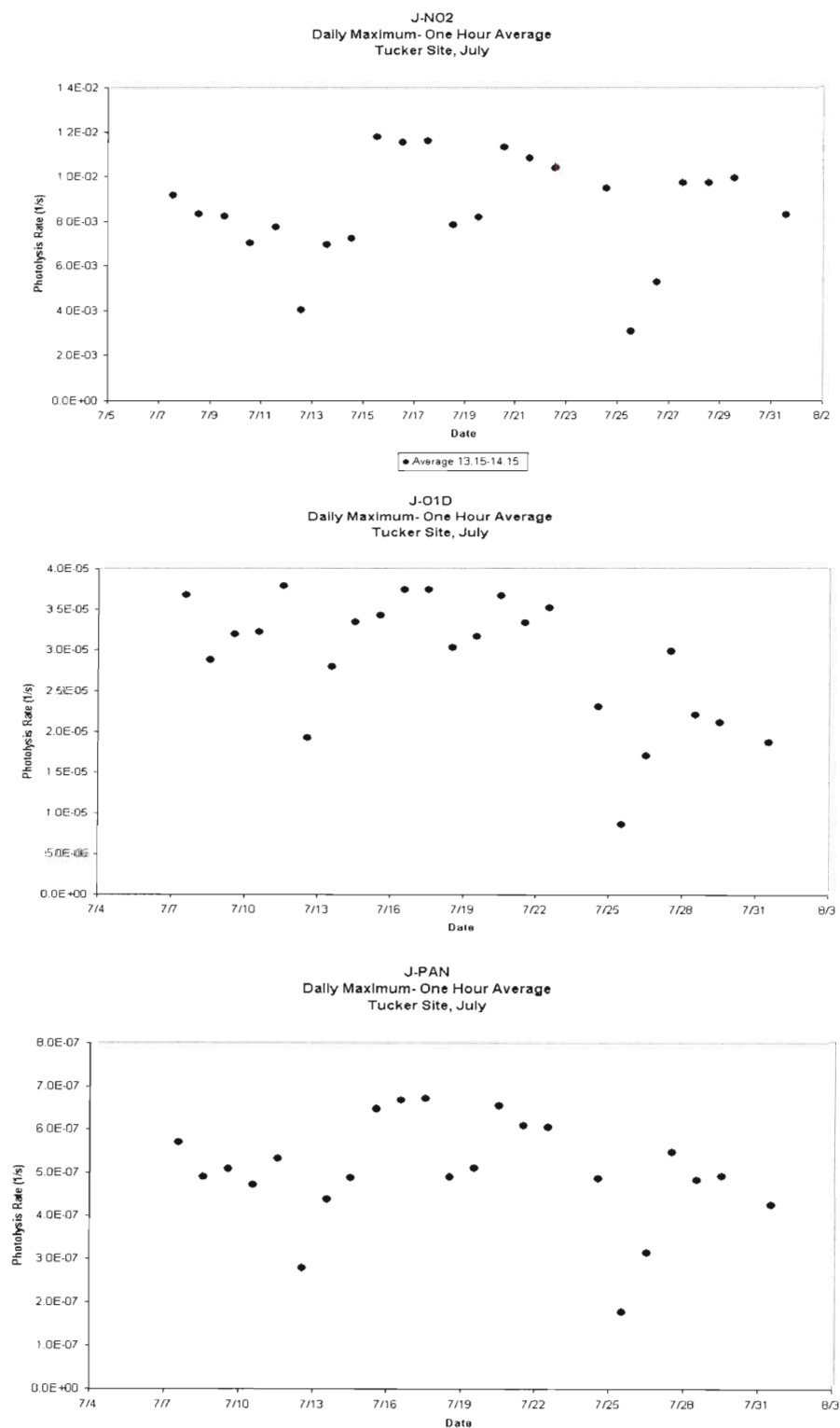
The TUV model calculates photolysis rates based on a cloud-free sky but most days are not free from at least a few clouds. Figure 19 below illustrates the daily variability in UV radiation at 350nm for a period of one week in July 2000. Every day during this week shows at least some cloud cover.



**Figure 19: Daily Variability of 350 nm Radiation**

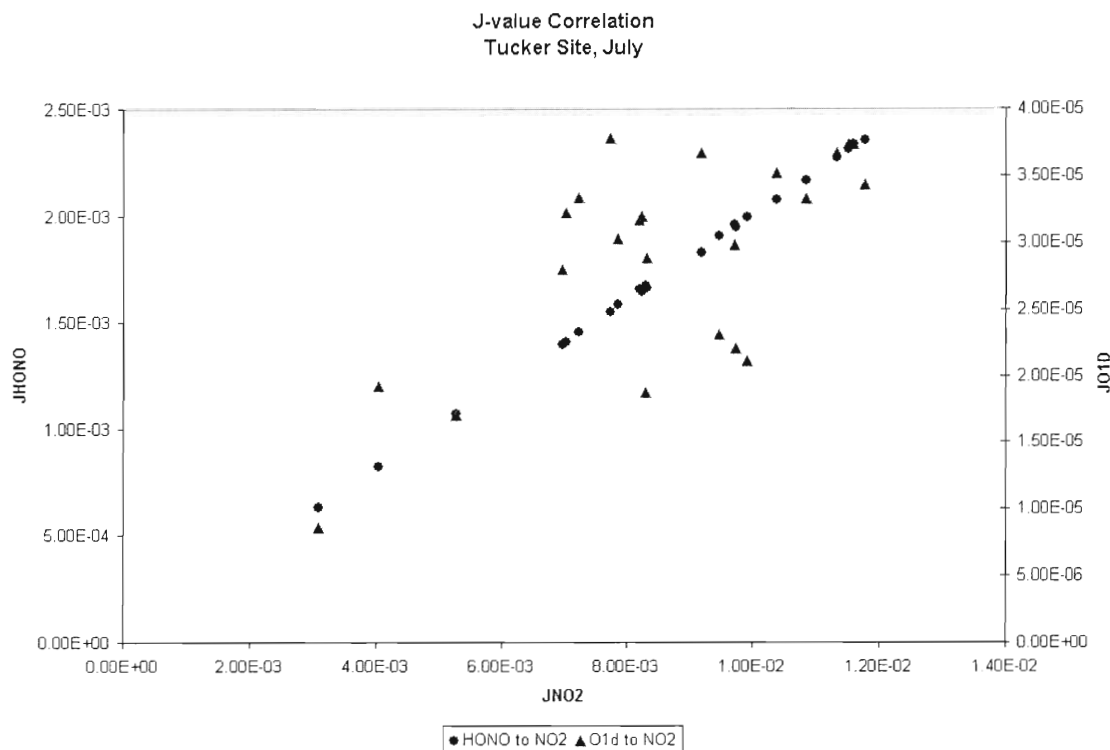


Figure 20 shows the variability in J-values for three photolysis rates;  $J(\text{NO}_2)$ ,  $J(\text{O}^1\text{D})$  and  $J(\text{PAN})$ . The data points represent one hour averages calculated at solar noon each day for the month of July.



**Figure 20: Variability of Photolysis Rates for Solar Noon During July 2000**

Figure 21 below shows the correlations of ozone and HONO photolysis rates with  $J(\text{NO}_2)$ . As expected,  $J(\text{HONO})$  and  $J(\text{NO}_2)$  show a good correlation since they have similar absorption wavelengths regions while  $J(\text{NO}_2)$  and  $J(\text{O1D})$  correlate more poorly since absorption occurs over a dissimilar interval.



**Figure 21: Correlation of Photolysis Rates**

### ***Measurement and Analysis Issues***

As shown in the previous section, the final photochemical rates determined by the prototype system were in excellent agreement with a variety of multi-stream radiative transfer models from both the National Center for Atmospheric Research and Georgia Tech. However, achieving this good agreement required substantial post processing of the UV spectra. Automated processing of the data often resulted in sub-optimal baseline correction of the spectra leading to artifacts such as negative photolysis rates. An example of such an artifact is shown below for an exceptionally clear day in August 2000 at the Tucker PAMS site.

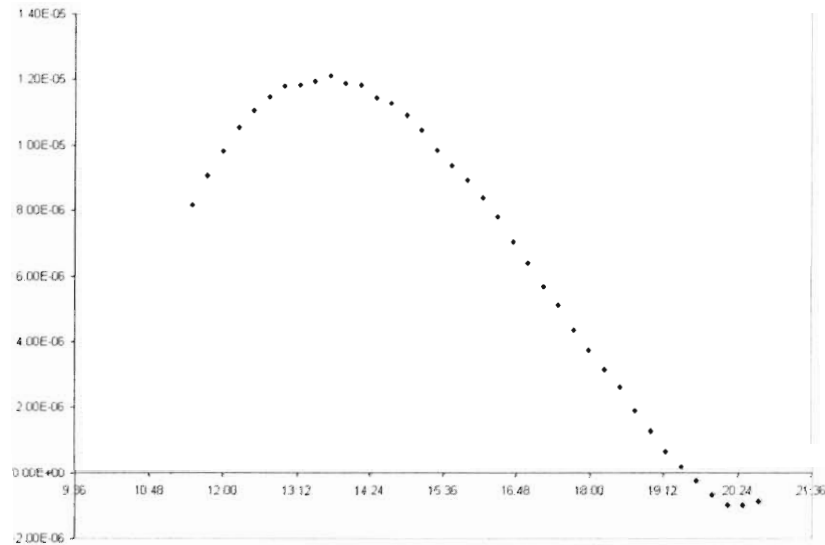


**Figure 22: J(O'D) for Tucker, GA with Baseline Artifact**

The presence of such artifacts resulted in substantially more data analysis activity that would be desirable for system making routine measurements. At present, the analysis/time ratio (that is the ratio of time to analyze the data to running time) is about 0.05. That is, it takes approximately one hour of analyst time to process and quality-assure twenty hours of data. For full time deployment this corresponds to about 0.2 FTE (full time equivalents) of personnel per measurement site. At an annualized cost including overhead of \$100k/technician year this corresponds to an annual cost of \$20,000 per site.

Another substantial operational difficulty is data handling. The prototype system produces in excess of 50 Mb of data storage per day of operations. While modern computer systems easily have the capacity to store this data, even for extended periods of operations, data transfer capabilities have not keep pace. Most PAMS and similar sites lack high-speed data connections and thus removable media normally provides data backup. Small capacity removable media are of limited usefulness for dealing with the large data volumes generated by the system and thus higher capacity (e.g. CD-R or DVD-R) devices are required. While these are readily available and media are inexpensive, “burning” a high capacity DVD requires substantial technician time and thus limits the number of sites that can be serviced. This limitation also imposes a significant personnel cost to operation of the instrumentation

## Conclusions and Recommendations

During 2001 and parts of 2002 additional tests were performed to optimize the instrumentation and procedures developed in the earlier test years. These modifications substantially improved the reliability of the hardware but resulted in less improvement in data analysis and reduction time. A summary of the principal finding and conclusions of the research program is given below:

- A reliable low cost and robust UV spectrophotometer based system for measurement of the most important photochemical rate coefficients has built and tested.
- The measurements from this system are in good agreement with modeling calculations under clear sky conditions and with other measurement methods.
- Data handling and data processing time remain issues. The system generates more 50 Mb of data/day and data cannot be conveniently transmitted over conventional telephone lines. Even weekly data pickup requires high capacity (CD-R or greater) storage media.
- The system can be deployed and maintained at low annualized costs, however, at present the cost of data analyst time (\$20,000/site/year) will need to be reduced in order to make such photolytic measurements are routine part of the PAMS network.
- While the inexpensive whole sky camera proved useful for the semi-quantitative measurements for which it was intended, it was found to lack sufficient dynamic range to be generally useful unless equipped with an automatic iris.



## References

- Bahe, F.C., W.N. Marx, U. Schurath and E.P. Roth, "Determination of the Absolute Photolysis Rate of Ozone by Sunlight,  $O_3 + h\nu = O(^1D) + O_2(^1\Delta_g)$ , at Ground Level" *Atmos. Env.*, Vol. 13, 1515-1522, 1979
- Bahe, F.C., U. Schurath and K.H. Becker, "The Frequency of  $NO_2$  Photolysis at Ground Level, as Recorded by a Continuous Actinometer" *Atmos Env*, Vol. 14, 711-718, 1980.
- Bairai, S.T. and D.H. Stedman, "Actinometer Measurements of  $J[O_3-O(^1D)]$  Using a Luminol Detector" Vol. 19, No. 20, 2047-2050, 1992.
- Bais, A.F., S. Madronich, J. Crawford, S.R. Hall, B. Mayer, M. van Weele, J. Lenoble, J.G. Calvert, C.A. Cantrell, R.E. Shetter, A. Hofzumahaus, P. Koepke, P.S. Monk, G. Frost, R. McKenzie, N. Krotkov, A. Kylling, W.H. Swartz, S. Lloyd, G. Pfister, T.J. Martin, E.-P. Roeth, E. Griffioen, A. Ruggaber, M. Krol, A. Kraus, G.D. Edwards, M. Mueller, B.L. Lefer, P. Johnston, H. Schwander, D. Flittner, B. G. Gardiner, J. Barrick and R. Schmitt, "International Photolysis Frequency Measurement and Model Intercomparison (IPMMI):Spectral Actinic Solar Flux Measurements and Modeling" *J. Geophys. Res.*, Vol. 108, D16, IPM 3, 2003.
- Blackburn, T.E, S.T. Bairai, and D.H. Stedman, "Solar Photolysis of Ozone to Singlet D Oxygen Atoms" *J. Geophys. Res.*, Vol. 97, No. D9, 10109-10117, 1992.
- Brauers, T., and A. Hofzumahaus, "Latitudinal Variation of Measured  $NO_2$  Photolysis Frequencies over the Atlantic Ocean between 50°N and 30°S" *J. Atmos. Chem.*, Vol. 15, 269-282, 1992.
- Calvert, J.G. and J.N. Pitts, Jr. "Photochemistry" John Wiley & Sons, Inc. 1966.
- Cantrell, C.A., J.G. Calvert, A. Bais, R.E. Shetter, B.L. Lefer and G.D. Edwards, "Overview and Conclusions of the International Photolysis Frequency Measurement and Modeling Intercomparison (IPMMI) Study" *J. Geophys. Res.*, Vol. 108, D16, IPM1, 2003.
- Castro, T., L.G. Ruiz-Suarez, J.C. Ruiz-Suarez, M.J. Molina and M. Montero, "Sensitivity Analysis of a UV Radiation Transfer Model and Experimental Photolysis Rates of  $NO_2$  in the Atmosphere of Mexico City" *Atmos Env.*, Vol. 31, No. 4, 609-620 1997.
- Castro, T., L.G. Ruiz-Suarez, M. Helguera, C. Gay and J.C. Ruiz-Suarez, "Experimental Determination of the Photolysis Constant of Nitrogen Dioxide for Mexico City" *International Conference on Air Pollution - Proceedings*, v 2, p 277-282, 1994.

Cotte, H., C. Devauz and P. Carlier, "Transformation of Irradiance Measurements into Spectral Actinic Flux for Photolysis Rates Determination" J. Atmos. Chem., Vol. 26, 1-28, 1997.

Crawford, J., R.E. Shetter, B. Lefer, C. Cantrell, W. Junkermann, S. Madronich and J. Calvert, "Cloud Impacts on UV Spectral Actinic Flux Observed During the International Photolysis Frequency Measurement and Model Intercomparison (IPMMI)" J. Geophys. Res., Vol. 108, D16, IPM 4, 2003.

Dahlback, A. and K. Stamnes, "A New Spherical Model for Computing the Radiation Field Available for Photolysis and Heating at Twilight" Space Sci., Vol. 39, No. 5, 671-683, 1991.

Degunther, M., and R. Meerkotter, "Influence of Inhomogeneous Surface Albedo on UV Irradiance: Effect of a Stratus Cloud" J. Geophys. Res., Vol. 105, No. D18, 22755-22761, 2000.

Dickerson, R.R., D.H. Stedman, W.L. Chameides, P.J. Crutzen and J. Fishman, "Actinometric Measurements and Theoretical Calculations of  $J(\text{O}_3)$ , the Rate of Photolysis of Ozone to  $\text{O}(^1\text{D})$ " Geophys. Res. Letters, Vol. 6, No. 11, 833-836, 1979.

Dickerson, R.R., D.H. Stedman and A.C. Delany, "Direct Measurements of Ozone and Nitrogen Dioxide Photolysis Rates in the Troposphere" J. Geophys. Res. Vol. 87, No. C7, 4933-4946, 1982.

Dickerson, R.R., S. Kondragunta, G. Stenchikov, K.L. Civerolo, B.G. Doddridge and B.N. Holben, "The Impact of Aerosols on Solar Ultraviolet Radiation and Photochemical Smog" Science, Vol 278, 10/31/97.

Duynkerke, P.G. and M. Van Weele, "Actinic Fluxes: The Role of Clouds in Photodissociation" Boundary-Layer Meteorology, Vol. 62, 417-432, 1993.

Edwards, G.D. and P.S. Monks, "Performance of a single-Monochromator Diode Array Spectroradiometer for the Determination of Actinic Flux and Atmospheric Photolysis Frequencies" J. Geophys. Res., Vol. 108, D16, IPM 5, 2003

Harvey, R.B., D.H. Stedman, and W. Chameides, "Determination of the Absolute Rate of Solar Photolysis of  $\text{NO}_2$ " J. of the Air Poll. Control. Assoc., Vol. 27, No. 7, 663-666, 1977.

Hofzumahaus, A., T. Brauers, U. Platt and J. Callies, "Latitudinal Variation of Measured  $\text{O}_3$  Photolysis Frequencies  $j(\text{O}^1\text{D})$  and Primary OH Production Rates over the Atlantic Ocean between 50°N and 30°S" J. Atmos. Chem., Vol 15, 283-298, 1992.

Hofzumahaus, A., A. Kraus, and M. Mueller, "Solar Actinic Flux Spectroradiometry: A Technique for Measuring Photolysis Frequencies in the Atmosphere" *Applied Optics*, Vol. 38, No. 21, 4443-4460, 1999.

Huey, J.W. "Experimental Determination of the Photolysis Rate Coefficients of Nitrogen Dioxide and Ozone" Thesis, Nov. 1993.

Junkermann, W., U. Platt and A. Volz-Thomas, "A Photoelectric Detector for the Measurement of Photolysis Frequencies of Ozone and Other Atmospheric Molecules" *J. Atmos. Chem.*, Vol. 8, 203-227, 1989.

Junkermann, W., "Measurements of the J(O1D) Actinic Flux within and Above Stratiform Clouds and Above Snow Surfaces" *Geophys. Res. Letters*, Vol. 21, No. 9, 793-796, 1994.

Kanaya, Y., Y. Kajii, H. Akimoto, "Solar Actinic Flux and Photolysis Frequency Determination by Radiometers and a Radiative Transfer Model at Rishiri Island: Comparisons, Cloud Effects, and Detection of an Aerosol Plume from Russian Forest Fires" *Atmos. Env.*, Vol. 37, 2463-2475, 2003.

Kazadzis, S., A.F. Bais, D. Balis and C.S. Zerefos, "Retrieval of Downwelling UV Actinic Flux Density Spectra from Spectral Measurements of Global and Direct Solar UV Irradiance" *J. Geophys. Res.*, Vol. 105, No. D4, 4857-4864, 2000.

Kjeldstad, B., B. Johnsen and T. Koskela, "Lamps as Means to Homogenize Solar Ultraviolet Irradiance Measurements Performed with Different Spectroradiometers" *J. Geophys. Res.*, Vol. 105, No. D4, 4787-4794, 2000

Kraus, A. and A. Hofzumahaus, "Field Measurements of Atmospheric Photolysis Frequencies for O<sub>3</sub>, NO<sub>2</sub>, HCHO, CH<sub>3</sub>CHO, H<sub>2</sub>O<sub>2</sub>, and HONO by UV Spectroradiometry" *J. of Atmos. Chem.*, Vol. 31, 161-180, 1998.

Kraus, A. F. Rohrer and A. Hofzumahaus, "Intercomparison of NO<sub>2</sub> Photolysis Frequency Measurements by Actinic Flux Spectroradiometry and Chemical Actinometry During JCOM97" *Geophys. Res. Letters*, Vol. 27, No. 8, 1115-1118, 2000.

Kylling, A., T. Persen, B. Mayer and T. Svenoe, "Determination of an Effective Spectral Surface Albedo from Ground-Based Global and Direct UV Irradiance Measurements" *J. Geophys. Res.*, Vol. 105, No D4, 4949-4959, 2000.

Landelius, T. and W. Josefsson, "Methods for Cosine Correction of Broadband UV data and Their Effect on the Relation Between UV Irradiance and Cloudiness" *J. Geophys. Res.*, Vol. 105, No. D4, 4795-4802, 2000.

Lantz, K.O., R.E. Shetter, C.A. Cantrell, S.J. Flocke and J.G. Calvert, "Theoretical, Actinometric, and Radiometric Determinations of the Photolysis Rate Coefficient of NO<sub>2</sub>

During the Mauna Loa Observatory Photochemistry Experiment 2" J. Geophys. Res., Vol. 101, No. D9, 14613-14629, 1996.

Madronich, S., "Photodissociation in the Atmosphere 1. Actinic Flux and the Effects of Ground Reflections and Clouds" J. Geophys. Res., Vol. 92, No. D8, 9740-9752, 1987.

Madronich, S., "Intercomparison of NO<sub>2</sub> Photodissociation and U.V. Radiometer Measurements" Atmos. Env. Vol. 21, No. 3, 569-578, 1987.

Madronich, S. and S. Flocke, The role of solar radiation in atmospheric chemistry, in *Handbook of Environmental Chemistry* (P. Boule, ed.), Springer-Verlag, Heidelberg, 1-26, 1998.

M. Muller, A. Kraus and A. Hofzumahaus, "O<sub>3</sub>-O(1D) Photolysis Frequencies Determined from Spectroradiometric Measurements of Solar Actinic UV-Radiation: Comparison with Chemical Actinometer Measurements" Geophys. Res. Letters, Vol. 22, No. 6, 679-682, 1995.

Okabe, Hideo, "Photochemistry of Small Molecules" Wiley-Interscience Publication, 1978.

Parrish, D.D., P.C. Murphy, D.L. Albritton and F.C. Fehsenfeld, "The Measurement of the Photodissociation Rate of NO<sub>2</sub> in the Atmosphere" Atmos. Env., Vol. 17, No. 7, 1365-1379, 1983.

Pfister, G., D. Baumgartner, R. Maderbacher, and E. Putz, "Aircraft Measurements of Photolysis Rate Coefficients for Ozone and Nitrogen Dioxide Under Cloudy Conditions" Atmos. Env. Vol. 34, 4019-4029, 2000.

Rossetti, G.H., E.D. Albizzati, and O.M. Alfano, "Modeling and Experimental Verification of a Flat-Plate Solar Photoreactor" Ind. Eng. Chem. Res. Vol. 37, 3592-3601, 1998.

Ruggaber, A., R. Dlugi, and T. Nakajima, "Modelling Radiation Quantities and Photolysis Frequencies in the Troposphere" J. Atmos. Chem., Vol. 18, 171-210, 1994.

Shetter, R.E., J.A. Davidson, C.A. Cantrell, N.J. Burzynski and J.G. Calvert, "Temperature Dependence of the Atmospheric Photolysis Rate Coefficient for NO<sub>2</sub>" J. Geophysical Res., Vol. 93, No. D6, 7113-7118, 1988.

Shetter, R.E., A.H. McDaniel, C.A. Cantrell, S. Madronich and J.G. Calvert, "Actinometer and Eppley Radiometer Measurements of the NO<sub>2</sub> Photolysis Rate Coefficient During the Mauna Loa Observatory Photochemistry Experiment" J. Geophys. Res. 10349-10359, 1992.



Shetter, R.E., C.A. Cantrell, K.O. Lantz, S.J. Flocke, J.J. Orlando, G.S. Tyndall, T.M. Gilpin, C.A. Fischer, S. Madronich and J.G. Calvert, "Actinometric and Radiometric Measurements and Modeling of the Photolysis Rate Coefficient of Ozone to O(1D) During Mauna Loa Observatory Photochemistry Experiment 2" J. Geophys. Res., Vol. 101, No. D9, 14631-14641, 1996.

Shetter, R.E., W. Junkermann, W.H. Swartz, G.J. Frost, J.H. Crawford, B.L. Lefer, J.D. Barrick, S.R. Hall, A. Hofzumahaus, A. Bais, J.G. Calvert, C.A. Cantrell, S. Madronich, M. Muller, A. Kraus, P.S. Monks, G.D. Edwards, R. McKenzie, P. Johnston, R. Schmitt, E. Griffioen, M. Krol, A. Kylling, R.R. Dickerson, S.A. Lloyd, T. Martin, B. Gardiner, B. Mayer, G. Pfister, E.P. Roth, P. Koepke, A. Ruggaber, H. Schwander and M. van Weele, "Photolysis Frequency of NO<sub>2</sub>: Measurements and Modeling During the International Photolysis Frequency Measurement and Model Intercomparison (IPMMI)" J. Geophys. Res., Vol. 108, D16, IPM 3, 2003.

Simpson, W.R., M.D. King, H.J. Beine, R.E. Honrath, and M.C. Peterson, "Atmospheric Photolysis Rate Coefficients During the Polar Sunrise Experiment ALERT2000" Atmos. Env. Vol. 36, 2471-2480, 2002.

Slusser, J., J. Gibson, D. Bigelow, D. Kolinski, P. Disterhoft, K. Lantz and A. Beaubien, "Langley Method of Calibrating UV Filter Radiometers" J. Geophys. Res., Vol. 105, No. D4, 4841-4849, 2000.

Stedman, D.H. and J.O. Jackson, "The Photostationary State in Photochemical Smog" 493-501, 1974.

Swartz, W.H., "Quantifying Photolysis Rates in the Troposphere and Stratosphere" Dissertation, Univ. Maryland, 2002.

Vasaras, A., A.F. Bais, U. Feister, C.S. Zerefos, "Comparison of two Methods for Cloud Flagging of Spectral UV Measurements" Atmos. Research, Vol. 57, 31-42, 2001.

Vuilleumier, L., J.T. Bamer, R.A. Harley, and N.J. Brown, "Evaluation of Nitrogen Dioxide Photolysis Rates in an Urban Area Using Data from the 1997 Southern California Ozone Study" Atmos. Env., Vol. 35, 6525-6537, 2001.

Webb, A.R., I.M. Stromberg, H. Li and L.M. Bartlett, "Airborne Spectral Measurements of Surface Reflectivity at Ultraviolet and Visible Wavelengths" J. Geophys Res., Vol. 105, No. D4, 4945-4948, 2000.

Webb, A.R., R.Kift, S. Thiel, and M. Blumthaler, "An Empirical Method for Conversion of Spectral UV Irradiance Measurements to Actinic Flux Data" Atmos. Env., Vol. 36, 4397-4404, 2003.

Weihs, P., A.R. Webb, S.J. Hutchinson and G.W. Middleton, "Measurements of the Diffuse UV Sky Radiance During Broken Cloud Conditions" J. Geophys Res., Vol. 105, No. D4, 4937-4944, 2000.

Wiegand, A.N. and N.D. Bofinger, "Review of Empirical Methods for the Calculation of the Diurnal NO<sub>2</sub> Photolysis Rate Coefficient" Atmos. Env., Vol. 34, 99-108, 2000.

Wild, O., X. Zhu and M.J. Prather, "Fast-J: Accurate Simulation of In- and Below-Cloud Photolysis in the Tropospheric Chemical Models" J. Atmos. Chem., Vol. 37, 245-282, 2000.

Wobrock, W. and R. Eiden, "Direct Solar Radiation: Spectrum and Irradiance Derived from Sun-Photometer Measurements" Applied Optics, Vol. 27, No. 11, 2253-2260, 1988.

Yu, S., V.K. Saxena, B.N. Wenny, J.J. DeLuisi, G.K. Yue and I.V. Petropavlovskikh, "A Study of the Aerosol Radiative Properties Needed to Compute Direct Aerosol Forcing in the Southeastern United States" J. Geophys. Res., Vol. 105, No. D20, 24739-24749, 2000.

Zafonte, L, P.L. Rieger and J.R. Holmes, "Nitrogen Dioxide Photolysis in the Los Angeles Atmosphere" Environ. Sci & Tech., Vol. 11, No. 5, 483-487, 1977

## Appendix: Typical TUV Model Conditions

Model Output for July 17<sup>th</sup> at 1300.

### INPUT PARAMETERS:

RADIATION SCHEME: 4 streams  
w-grid: 141 120. 735.  
z-grid: 81 0.300000012 80.3000031  
measurement point: index 1 altitude= 0.300000012  
DATAE1/SUN/susim\_hi.flx  
DATAE1/SUN/atlas3\_1994\_317\_a.dat  
DATAE1/SUN/neckel.flx  
air temperature: USSA, 1976  
air density: USSA, 1976  
old sea level air column = 2.1518E+25 # cm-2 = 1014.94 mbar  
new sea level air column = 2.1518E+25 # cm-2 = 1014.94 mbar  
surface air column = 2.0790E+25 # cm-2 = 980.59 mbar  
ozone profile: USSA, 1976  
old O3 Column = 9.3520E+18 # cm-2 = 348.05 Dobson Units  
new O3 Column = 8.0610E+18 # cm-2 = 300.00 Dobson Units  
SO2: 1 ppb in lowest 1 km, 0 above  
old SO2 Column = 1.8830E+15 # cm-2 = 0.07 Dobson Units  
new SO2 Column = 0.0000E+00 # cm-2 = 0.00 Dobson Units  
NO2: 1 ppb in lowest 1 km, 0 above  
old NO2 Column = 1.8830E+15 # cm-2 = 0.07 Dobson Units  
new NO2 Column = 0.0000E+00 # cm-2 = 0.00 Dobson Units  
Cloud: 4levels, tot opt. dep. = 0.  
aerosols: Elterman (1968)  
Total aerosol od at 340 nm = 0.328121424  
wavelength-independent albedo = 0.150000006  
idate = 717 esfact = 0.967483699  
lat= 33.8482018 long= -84.2142029 ut= 13.  
solar zenith angle = 62.8823967

### PHOTOLYSIS RATES (1/sec):

1 O2 + hv -> O + O 0.000E+00  
2 O3 -> O2 + O(1D) 5.611E-06  
3 O3 -> O2 + O(3P) 3.368E-04  
4 NO2 -> NO + O(3P) 5.461E-03  
5 NO3 -> NO + O2 1.851E-02  
6 NO3 -> NO2 + O(3P) 1.418E-01  
7 N2O5 -> NO3 + NO + O(3P) 8.946E-12  
8 N2O5 -> NO3 + NO2 1.906E-05  
9 N2O + hv -> N2 + O(1D) 0.000E+00  
10 HO2 + hv -> OH + O 0.000E+00  
11 H2O2 -> 2 OH 2.981E-06  
12 HNO2 -> OH + NO 1.156E-03  
13 HNO3 -> OH + NO2 1.937E-07  
14 HNO4 -> HO2 + NO2 1.442E-06  
15 CH2O -> H + HCO 1.165E-05  
16 CH2O -> H2 + CO 2.201E-05  
17 CH3CHO -> CH3 + HCO 1.437E-06  
18 CH3CHO -> CH4 + CO 4.382E-14  
19 CH3CHO -> CH3CO + H 0.000E+00  
20 C2H5CHO -> C2H5 + HCO 5.812E-06  
21 CHOCHO -> products 4.986E-05

22 CH<sub>3</sub>COCHO -> products 6.726E-05  
23 CH<sub>3</sub>COCH<sub>3</sub> 1.604E-07  
24 CH<sub>3</sub>OOH -> CH<sub>3</sub>O + OH 2.382E-06  
25 CH<sub>3</sub>ONO<sub>2</sub> -> CH<sub>3</sub>O+NO<sub>2</sub> 2.716E-07  
26 PAN + hv -> products 2.650E-07